7-15-2011

Extremal Reaches in Polynomial Time

Ciprian S. Borcea
Rider University

Ileana Streinu
Smith College, istreinu@smith.edu

Extremal Reaches in Polynomial Time [*]

Ciprian S. Borcea
Department of Mathematics
Rider University
Lawrenceville, NJ 08648, USA
borcea@rider.edu

Ileana Streinu
Department of Computer Science
Smith College
Northampton, MA 01063, USA
istreinu@smith.edu

ABSTRACT

Given a 3D polygonal chain with fixed edge lengths and fixed angles between consecutive edges (shortly, a revolute-jointed chain or robot arm), the Extremal Reaches Problem asks for those configurations where the distance between the endpoints attains a global maximum or minimum value. In this paper, we solve it with a polynomial time algorithm.

Categories and Subject Descriptors

F.2.2 [**Analysis of algorithms and problem complexity**]: Non-numerical algorithms and problems—*Geometrical problems and computations*

General Terms

Algorithms, Theory

Keywords

robot arm, reach problem

1. INTRODUCTION

We present the first polynomial time algorithms for the Maximum and Minimum Reach problems: given a 3D polygonal chain with fixed edge lengths and fixed angles between consecutive edges (shortly, a revolute-jointed chain or robot arm), find configurations where the distance between the endpoints is extremal (absolute maximum or minimum), and continuously reconfigure the chain to attain such an extremum.

To put the problems in their proper context, we have to introduce a more general concept which includes the polygonal chain as a special case.

Revolute-jointed chains. Whenever we open an ordinary door, we see a *revolute joint* in operation: one body (the door) can rotate with respect to another (the wall),

with the two bodies remaining attached along a common *hinge*. When this type of connection is used repeatedly for articulating, one after another, a series of rigid bodies, the result is a revolute-jointed robot arm, or, in more geometric language, a *body-and-hinge chain*, illustrated in Fig. 2(c). The terminology in robotics uses *link* for a body and *joint* or *turning axis* for a hinge. A revolute-jointed robot arm is also called a serial manipulator with revolute joints. We emphasize from the beginning that *our geometric models have no rotational limitations around the hinges and no self-collision prohibitions.*

General kinematic properties of robot arms are normally investigated under these 'ideal' assumptions not only for the sake of theoretical coherence or uniformity but also as a benchmark level for evaluating the arm's capabilities before implementing 'practical' limitations resulting from specific execution decisions and available technologies. For any given 'ideal' structure self-collision issues are obviously dependent on the particular physical execution of the robot arm. It may be mentioned here that shape designs which avoid physical self-collision are always possible.

Under our 'ideal' assumptions, the shape of the bodies making the chain is irrelevant. What matters is the relative position of the two hinges incident to each intermediate body. Chains where the two hinges incident to each body are coplanar are called *panel-and-hinge chains*. A *panel* is, in this case, the plane spanned by two consecutive hinges. The first (as well as the last) body is incident to only one hinge and an endpoint, which together determine the first (respectively the last) panel.

In Fig. 1(a) we show the type of robotic arm primarily considered in this paper, arising from a 3D polygonal chain with fixed edge lengths and fixed angles between consecutive edges. The plural form means that, while each edge maintains its length, different edges may have different lengths and similarly for angles: the angle between two consecutive edges does not vary, but need not be the same for one pair of consecutive edges and another. The fixed angle between two rigid edges creates a rigid triangle, and thus the polygon can be conceived as a chain of rigid panels. See Fig. 1(b). The polygon edges, except the two extreme ones, act as hinges between two consecutive panels. Polygonal chains can therefore be treated as generic panel-and-hinge chains.

Extremal Reaches. The first body (the *base*) is considered fixed, and the last body carries the *end-effector* or *hand* of the robot which is abstracted as a marked point T. When a point S is marked on the first body, we have two 'ends' (see Fig. 2(c)). The distance between S and T, as the
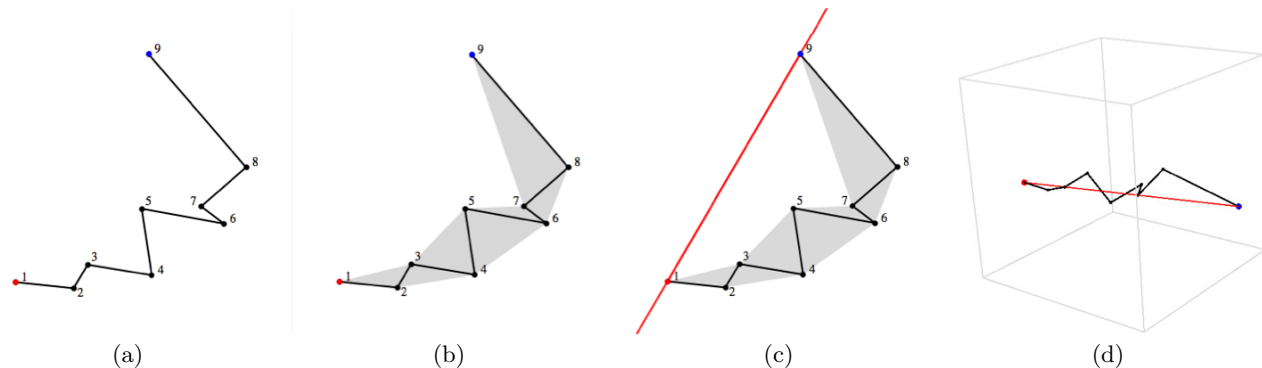
Figure 1: (a) A general polygonal chain, viewed in a standard (zigzag) flat configuration. (b) The polygon, turned into a panel-and-hinge chain. All the edges of the polygon, except the two extreme ones, act as hinges (revolute joints) and allow for hinge-like rotations of the two incident triangles (gray panels). (c) The endpoint axis, illustrated for the zigzag flat configuration. (d) A corresponding 3D max reach configuration of the same chain, as calculated by the algorithm from [6].

chain adopts various configurations, induces the *end-to-end distance function*. It takes a continuum of values between a certain *minimum*, which may be zero or non-zero, and a certain *maximum*. The **extremal reaches problem** for a given body-and-hinge chain asks for the determination of these two values and of configurations achieving them.

A zero minimum means that T can reach the base-point S. Finding the configurations with $S = T$ is an instance of the fundamental *inverse kinematics problem* described in any robotics textbook (e.g. [14]). For a generic robot arm with $n \geq 4$ revolute joints, the solution space of this inverse kinematics problem has dimension $n-3$. On the other hand, a non-zero minimum means that S cannot be reached and the minimum reach configurations will be, generically, isolated and therefore in finite number. *This sharp contrast is the reason for setting apart the zero-minimum case, which is not addressed in this paper.*

Problem History and Importance. The extremal reaches problem is fundamental in robotics, where it appears in robot design, placement in the environment, motion planning and performance evaluation. Robotic manipulators are expensive mechanical objects, often designed for specific tasks. Many practical robot arms have relatively few degrees of freedom (dofs), usually up to 6. Six degrees of freedom are enough for performing locally any 3D rigid transformation on objects held by the end-effector. Robot arms with more than six degrees of freedom are called redundant. One example is the Canadarm2 robotic manipulator operating on the space station: it has seven revolute joints and hence 7 dofs [12]. But recent applications are bringing to the forefront the so-called hyper-redundant robots, with large number of joints. In all these cases, the specifications of the manipulator must include its *reachability region*, or *workspace*.

The relevance of extremal reaches for the *workspace determination problem* has been recognized since the early days of robotics [11, 15, 19]. An ACM best thesis award [10] was given 25 years ago for an approximate computational method. Models of articulated body-and-hinge structures (from human limbs to snakes and caterpillars) appear abundantly not only in the industrial applications of robotic manipulators, but also in biologically inspired robotics, robots

in surgery, nano-robotics, video game design, computer graphics and animation. Most importantly, formulations based on robot arm kinematics are applied to molecular conformations, in particular protein structures (see e.g. [7, 20]), and the end-to-end length of a protein is a significant parameter in mechanical unfolding and refolding experiments [13].

Although both extremal values are important, virtually all previous investigations focused on the maximum reach. A necessary condition, satisfied by all critical points of the end-to-end (squared) distance function (points where the differential is zero, which include the extrema) was identified in the early 1980's [9, 11, 16, 19]. However, the number of critical points increases exponentially with the number of joints and the absence of a criterion for distinguishing maxima and minima among them hampered computational advances: neither gradient-based optimization nor Monte Carlo sampling guarantee the correctness or accuracy of their "solutions". Moreover, the numerical methods do not scale up for large chains, as demanded by modern applications in nano-robotics or sampling of protein conformation spaces.

In the computational geometry literature, a restricted version of the problem appeared in the 2001 PhD thesis of Soss at McGill University [17], who looked at the minimum and maximum among all *flat configurations* of polygonal chains with fixed edge lengths and fixed consecutive angles, and showed these problems to be NP-hard. A formulation as an optimization problem, and an analysis of the resulting numerical approximation method is also presented in Chapter 6 of this thesis. This led to the conjecture stated in [8], p. 135, that the 3D version would also be NP-hard.

Recent contributions. Our recent theoretical results [5], provide a complete characterization of the maximum reach for body-and-hinge chains and a complete characterization of the non-zero minimum reach for panel-and-hinge chains. We remind the reader that a panel-and-hinge chain is a body-and-hinge chain which has any two consecutive hinges in the same plane. A *generic* panel-and-hinge chain has intersecting consecutive hinges, with no more than two hinges incident in one point. The non-generic ones may have

(a)

(b)

(c)
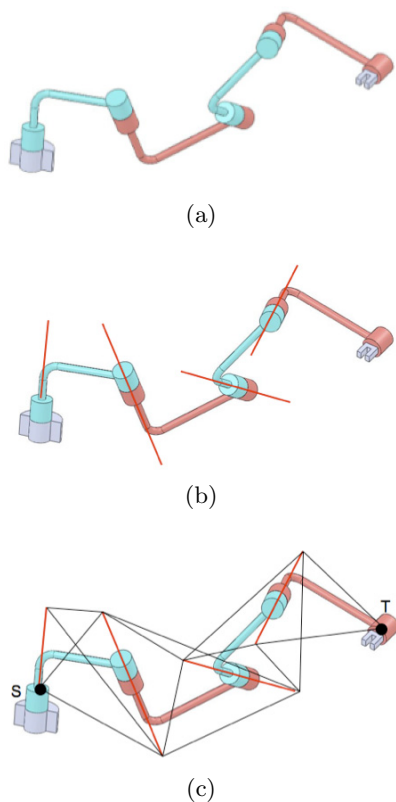
Figure 2: (a) A general revolute-jointed robotic arm. One end is a grounded base and the other is called an end-effector. (b) The red hinge-axes (revolute joints) allow for hinge-like rotations. (c) The robotic arm viewed as a body-hinge chain: a series of rigid bodies (shown as tetrahedra) connected along the red hinges, which allow rotations of one body relative to the neighboring one. The start point S on the base and the terminus point T on the end-effector are shown.

parallel hinges, or several hinges incident in one point. By retaining, on each hinge, only the segment between the intersection with its neighboring hinges and by joining S to a point on the first hinge and T to a point of the last hinge, a generic panel-and-hinge chain is equivalently represented as a *polygonal chain* with fixed edge lengths and fixed angles between consecutive edges. This is the model used by most computational geometers who investigated revolute-jointed robot arm problems [2, 3, 18]. When all the fixed angles are equal to $\frac{\pi}{2}$, we have an *orthogonal chain*.

In [6] we have shown that our theoretical characterizations have important computational implications by giving *optimal linear time algorithms* for the maximum reach problem of a class of polygonal chains (characterized by a technical property). This class will be referred to, from now on, as *zigzag foldable polygons*. It includes the easier-to-define orthogonal chains, used in our previous papers as an alias for the larger class. See Fig. 1(d) for an example of such a zigzag foldable polygon which is not orthogonal. More recently, we also obtained a linear time algorithm for the minimum reach problem on zigzag foldable chains. This is the basis for the

theory and efficient algorithms developed in [4] for tracing the precise workspace boundary of orthogonal chains.

The complete solution of the orthogonal case and the strong combinatorial character of the theoretical criterion for extremal configurations in the panel-and-hinge case, led to our conjecture [6] on the possibility of polynomial time algorithms for computing the extremal reaches of panel-and-hinge chains.

Results. *In this paper, we settle the polynomial time complexity for the Extremal Reaches Problem of arbitrary polygonal chains.* We first prove a *new* structural theorem, valid for *all* polygonal chains, which characterizes flat maxima in terms of an *empty ellipse criterion*. Our algorithms are easy to implement and have immediate applications to workspace determination problems in robotics or computing geometric parameters of protein backbones in bio-geometry.
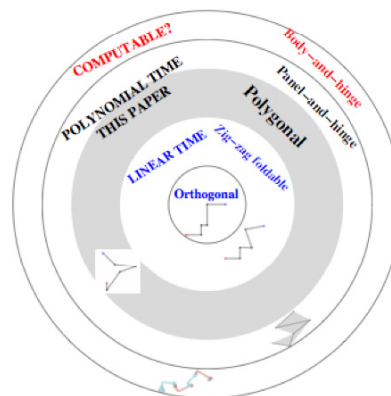
Figure 3: Geometric and algorithmic classification of revolute-jointed robot arms.

As in [6], the algorithms apply to three types of questions:

1. **Extremal Reach Value:** compute the maximum, resp. minimum value of the endpoint distance function.

2. **Extremal Reach Configurations:** compute one (or enumerate all) of the configurations that achieve the global maximum, or global minimum endpoint distance, when this value is not zero.

3. **Path Planning:** given an arbitrary configuration of the chain, reconfigure it to an extremal reach position, when not zero; i.e. compute a trajectory in configuration space ending at the extremal reach configuration.

The main effort (and the focus of this paper) goes into the second problem. Once an extremal reach configuration has been computed, it yields the extremal value, and it contains the necessary information for computing the folding (dihedral) angles that induce a path in configuration space using classical forward kinematics techniques. We remark that our results extend to arbitrary panel-and-hinge chains (not necessarily the generic ones arising from polygonal chains).

A key element in our proofs is an *empty ellipse criterion* for flat maxima. It is reminiscent of other distinctive structures in Computational Geometry, such as the empty circle
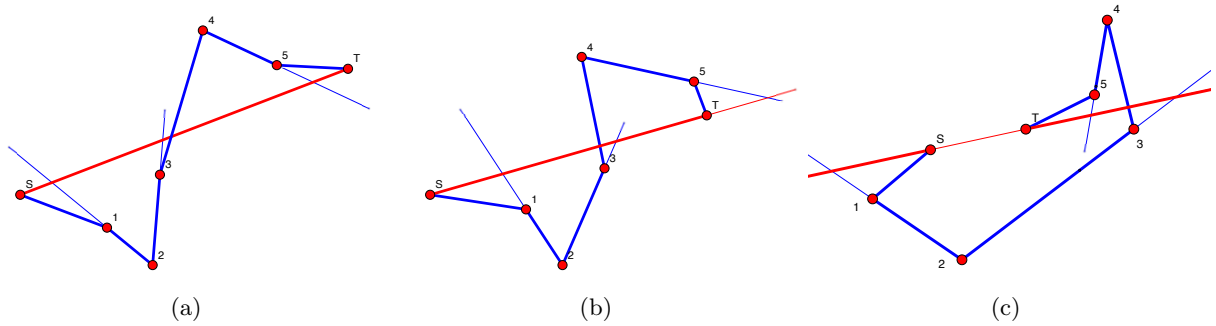
Figure 4: Illustration of the *natural order* criterion for maximum, resp. minimum reach of polygonal chains. Extensions of the thick hinge segments are shown with thinner lines. **(a)** This flat chain is in its global maximum position, since the oriented segment ST crosses the hinges in the natural order. **(b)** The hinges are crossed here in a different order: this flat configuration, although a critical one for the endpoint distance function, is not a maximum. **(c)** A configuration in a flat non-zero minimum: the oriented projective complement of ST is crossed by the hinges in natural order.

property of Delaunay triangulations. We use it to develop a procedure for "merging" recursively the solutions obtained for subchains, in a dynamic programming fashion. Another new theoretical tool introduced here is a form of projective duality, in the panel-and-hinge case, between maximum and minimum reaches. It turns the ellipse in the *empty ellipse criterion* into a hyperbola, and leads to an extension of the maximum reach algorithm to solve the minimum reach. This is a context specific occurrence. The combinatorial characterization of [5] for minima of panel-and-hinge chains does not carry over to minima for the body-and-hinge case, indicating that the minimum reach may be substantially more difficult than the maximum reach. Likewise, the linear time algorithm for maxima of orthogonal chains [6] does not carry over to the case of minima, which requires non-trivial ideas in order to stay within the same complexity class [4].

2.   DEFINITIONS

A polygonal chain in $3D$ with n revolute joints (hinges) is denoted by $p = \{p_0, p_1, \cdots, p_{n+2}\}$, and assumed to have fixed edge lengths and fixed angles between consecutive edges. The hinges correspond to the internal edges $e_i = (p_i, p_{i+1})$, $i = 1, \cdots, n$. The two points p_0 and p_{n+2} are referred to as the *endpoints* of the chain, with $S = p_0$ being the *start* or *origin*, and $T = p_{n+2}$ the *terminus* or *end point*. The example in Fig. 1 has $n = 6$ hinges. Another way to look at a revolute-jointed polygonal chain is as follows: the fixed angle constraint turns all triplets of vertices $p_i p_{i+1} p_{i+2}$ into rigid triangles, since the length of the edge $p_i p_{i+2}$ is implied by the other two and the angle between them. The plane of the triangle is called a *panel*, and consecutive panels $p_i p_{i+1} p_{i+2}$ and $p_{i+1} p_{i+2} p_{i+3}$ are joined by the hinge e_{i+1} running through $p_{i+1} p_{i+2}$. Occasionally, we may use indices, such as i, to refer to the point p_i, or designate the intersection of two consecutive hinges A_i and A_{i+1} by $p_{i,i+1} = p_{i+1}$. We **emphasize** that *a hinge should be conceived as an entire line, not just a line segment.*

The set of all possible spatial positions of the vertices which satisfy the edge length and angle constraints of a revolute-jointed chain, *up to rigid motions*, forms the *configuration space* of the chain. When all the panels are coplanar, we say that the panel-and-hinge structure is *in a flat*

configuration or simply *flat*. If the panels arise as triangles from a revolute-jointed polygonal chain, a special *standard* or *zigzag* configuration is distinguished, where two consecutive triangle do not overlap. Equivalently, the polygonal chain turns, alternately, left or right at consecutive vertices. Figures 1(a,b,c) show a chain with 6 hinges in its zigzag *flat configuration*, while the chains in Fig. 4 are not in zigzag configurations.

The *endpoint axis* is the line through S and T. It is divided into two pieces: the finite segment $[ST]$ (the *endpoint segment*) and its *projective complement* $]ST[$, consisting of two infinite rays, thought of as connected by a projective *point at infinity*. These "segments" are oriented: $[ST]$ is oriented in the usual way, from S to T, and the projective complement $]ST[$ is oriented from S, away from T towards infinity, and then, on the other ray, back from infinity towards T.
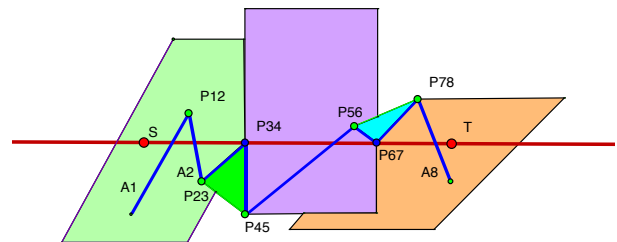
Figure 5: A panel-and-hinge chain in a 3D maximum reach configuration. The segment from S to T intersects all hinges in their sequential order. There are two fold points, at p_{34} and p_{67}, three flat pieces and two folding panels, each induced by the pair of hinges incident to a fold point.

The *end-to-end* or *endpoint distance function* assigns a real non-negative value, the distance between the endpoints S and T, to each spatial configuration of the chain. In fact, the squared distance function is more convenient for computations. The endpoint distance varies between two extreme values, the *global* minimum and maximum, with the possibil-

ity of various other local minima, maxima, or other critical values of the squared endpoint function.

It is known [9, 11, 16, 19] that in all critical configurations, the endpoint *axis* meets all the hinges. When applied to polygonal chains, three cases are distinguished: the endpoint axis meets hinge i (line through p_i and p_{i+1}) either inside the segment $p_i p_{i+1}$, outside it, or at one of the endpoints. Two or more consecutive hinges cut by the endpoint axis away from their intersection point must be coplanar: the panels between them are folded over in a flat configuration. This leads to a structural decomposition of a polygonal (panel-and-hinge) chain (in a critical configuration), into (a) flat pieces and (b) fold points. The flat pieces arise from contiguous segments of the chain (i.e. within an interval i to j of vertex indices), in which several coplanar consecutive hinges are cut (simultaneously, in their common plane) by the endpoint axis. The flat pieces are connected at fold points, which are those vertices of the polygon which meet the endpoint axis. The two hinges incident at each fold point determine, in addition, a simpler "triangular" *folding panel*, which is met by the endpoint axis only at the fold point. These concepts are further illustrated with 3D examples in [6]. They can also be observed in the 3D maximum reach configuration from Fig. 1(d), although the 2D rendering of 3D space makes it more difficult to "see" the geometry. Fig. 5 sketches this structural decomposition.

3. IDENTIFYING FLAT MAXIMA

The *natural order* of the hinges is $1, 2, 3, \cdots$ as they appear on the chain. In [5], we proved that a body-and-hinge chain is in a *global maximum configuration* if and only if the *oriented segment* $[ST]$ intersects all hinges *in their natural order*. We also proved that for *panel-and-hinge* chains, a non-zero minimum reach configuration has the property that the oriented projective complement $]ST[$ of $[ST]$ meets the hinge axes in the natural order. This leads, in particular, to a simple *verification method* for flat extrema, illustrated with a few examples in Fig. 4.

A *dual characterization* of the global maximum as a constrained shortest-path is also proven in [5]: *The global maximum of the endpoint distance function coincides with the length of the* shortest path *from S to T which meets all hinges in their natural order*. This result allowed us to recast the reach calculation as a constrained shortest path problem. In [6], we identified those polygonal chains where this constrained shortest path can be computed from the standard zigzag configuration. In this case, an additional, very special property holds: the endpoint axis cuts through all the polygon *segments*, i.e. it meets the hinges in the interior of their defining polygon segment, not outside. The algorithm we gave in [6] works by finding a shortest path from S to T constrained to lie inside the *paneled polygon*, which is the union of all triangular panels, in the flat zigzag position (see Fig. 1(b)). The shortest path is a polygonal line: its intermediate vertices become the fold points of the final max reach configuration. The panels crossed by the shortest path segments become *frozen* to form a larger flat panel. Viewed in isolation, as a smaller chain, the subchain between two fold points attains a flat maximum in its zigzag configuration. This is the reason we have chosen the name *zigzag foldable* polygons for the class on which our previous algorithm works, as referred to in the introduction and in Fig. 3.

The final ingredient was a lemma stating under which conditions the frozen panels, now forming themselves a panel-and-hinge chain, can be folded in 3D, around the hinges incident to the fold points, to allow for the shortest path to *straighten* in 3D. These conditions (related to the triangle inequality on the sphere) are always satisfied for orthogonal chains. Fig. 1 shows a non-orthogonal example where this approach works (in other words, the example in Fig. 1 is a zigzag foldable polygon), and it is not difficult to produce examples where it fails (such as Fig. 6(a)).

The chains for which the previous algorithm yields non-foldable vertices on the shortest path from S to T contain subchains which *attain their maxima in flat but not zigzag configurations* (see Fig. 6(a)). The characterization and identification of these non-standard subchain maxima remains the main difficulty to overcome. We do it in two steps. First, we handle the basic case of chains with no more than two hinges. Then we show how to identify larger flat chains from smaller flat ones.

Contextual comparison with previous approaches. It is instructive, at this point, to comment on our results in the context of previous work. Soss [17] proved that finding the maximum (resp., minimum) among all *flat configurations* is NP-complete. What is the relationship between his NP-hardness result, and our polynomial time algorithm for flat maxima? The difference is that Soss' problem asks for the maximum over a smaller set of configurations, and that maximum may *not* be a *maximum* over all 3D configurations. In our case, when we *know* a priori that the maximum is flat, we use the additional structure given by the empty ellipse criterion. Without it, we would be reduced to trying all flat folding patterns, which are exponentially many.

3.1 The case of two hinges: fold points and flat patterns

Critical configurations of panel-and-hinge chains are, as we indicated, subdivided into flat pieces connected at *fold points*. A fold point must be located at the intersection of two consecutive hinges. A local condition (the *antipodal triangle inequality*), satisfied by three special angles traced on the flat pieces at a fold vertex, has been derived in [6] as a criterion used for identifying the fold vertices of (in this paper's terminology) the maximum reach configurations of zigzag foldable polygonal chains. In [4], this is supplemented with a criterion for minimum reach, which is a spherical triangle inequality.

This leads to the following small **subroutine** (which we call the **two-hinge rule**) for identifying the folding patterns of extremal reach configurations for chains $p_0 p_1 p_2 p_3 p_4$ with two hinges, in constant time: (a) Calculate the three relevant angles, $\angle p_0 p_2 p_1$, $\angle p_1 p_2 p_3$ and $\angle p_3 p_2 p_4$, as in [6]; (b) Test if they satisfy the spherical triangle inequality. If so, the minimum reach of the chain is attained in a 3D position, where the three panels fold, allowing the alignment in 3D of the segments $p_0 p_2$ and $p_4 p_2$, by rotations about hinges $p_1 p_2$ and $p_3 p_2$ incident to the fold vertex p_2; (c) Test for the antipodal triangle inequality, to see if the Max Reach is attained in a 3D position. If so, the maximum reach of the chain is attained in a 3D position, where the three panels fold, allowing the alignment in 3D of the two line segments $p_0 p_2$ and $p_4 p_2$, by rotations about hinges $p_1 p_2$ and
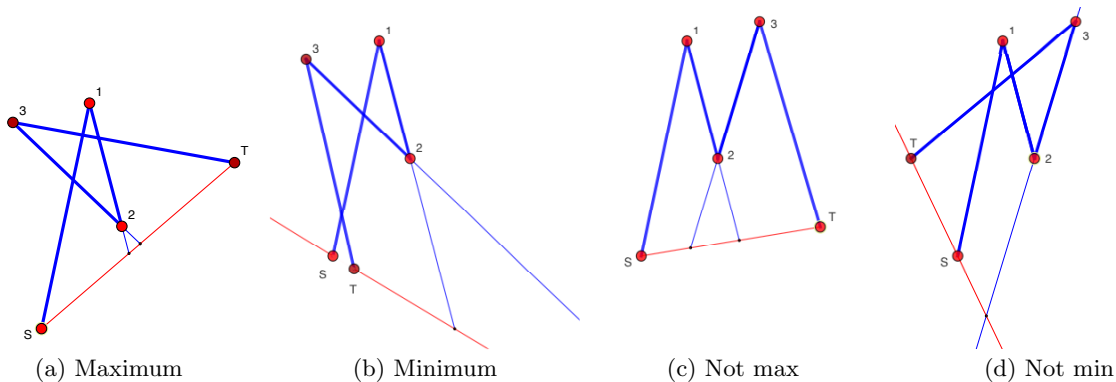
Figure 6: **Four patterns of folding a** 2**-hinge chain which achieves both max and min reaches in flat positions.**

$p_3 p_2$ incident to the fold vertex p_2. Finally: (d) Check all the four flat positions, as in Fig 6, for flat extrema. We will use this subroutine in our main algorithms.

Fig. 6 shows the four possible ways in which a 2-hinged chain can fold flat: in the case illustrated here, both the maximum and minimum reach are achieved in flat positions.

3.2 The Empty Ellipse Property

We turn now to our new criterion for flat maxima. Let us consider a polygonal chain whose maximum reach is attained in a flat (not necessarily zigzag) configuration. We denote it by ST (not to be confused with the endpoint axis, or the endpoint segment $[ST]$). For an arbitrary vertex of the polygon P, we denote by SP, resp. PT, the two subchains from S to P, resp. from P to T. If the subchains SP and PT are in flat configurations, then they induce a short (three panels and two hinges) panel-and-hinge chain consisting of the flat configuration of SP, the panel between the two hinges incident at P, and the flat configuration of PT. We say that we apply the *two-hinge rule* to this two-hinge chain, when we determine its maximum reach, according to the subroutine described above in Section 3.1.

In the sequel, by a *proper vertex* of a polygonal chain, we mean one which is the intersection of two hinges, i.e. we exclude p_0, p_1, p_{n+1} and p_{n+2}. The main theoretical result of the paper can now be stated.

THEOREM 3.1. **(Empty Ellipse Property)** *Consider a polygonal chain from S to T which attains its maximum reach in a flat configuration C. Let P be a proper polygon vertex with the property that, in this maximal configuration C, the ellipse with foci at S and T, going through P, contains, in its interior, no other proper vertices of the polygonal chain in configuration C. Then the subchains SP and PT are also in flat maximal configurations.*

Let $|SP|$ and $|PT|$ denote the distance between S and P, respectively P ant T in the maximal flat configuration C. Then, for any other proper vertex Q, we have:

$$|SP| + |PT| \leq Max\{SQ\} + Max\{QT\} \qquad (1)$$

where $Max\{SQ\}$ and $Max\{QT\}$ denote the maximum reach of the subchain SQ, respectively QT.

PROOF. It is a simple observation that when the maximum reach configuration is flat, then it is (generically) unique. Indeed, when there are f fold vertices, the number of configurations is 2^f [5]. In a flat maximum reach configuration, let $P = p_{i+1}$ be a proper vertex with the property that the sum of the lengths of the two segments $[SP]$ and $[PT]$ be minimal among such sums. Then the ellipse with foci at S and T, going through P, is empty of all other proper polygon vertices p_j, $j = 2, \cdots, n$. Indeed, the ellipse is the locus of points with a given distance sum to the two foci, and for points inside the ellipse, this sum decreases.

Let us denote by A_k the kth hinge of the chain, in this flat maximum reach position, i.e. the line through points p_k and p_{k+1}, for $k = 1, \cdots, n$. Fig. 7(a) illustrates the argument, which goes as follows.

Because the configuration is a maximum reach, the segment from S to T intersects all hinges in the natural order in points $a_k = [ST] \cap A_k$. But then these same hinges, for $k < i$, will intersect the segment from S to P in the natural order in points $b_k = [SP] \cap A_k$, for otherwise we would have a consecutive hinge crossing inside the ellipse. Similarly, for $i + 1 < j$, the hinges A_j intersect the segment from P to T in the natural order. Applying our Maximum Reach criterion, it follows that we have a flat maximum reach SP for the initial sub-chain of the first i panels and a flat maximum reach PT for the terminal sub-chain of the last $n - i$ panels. Moreover, the maximum reach for the full chain and for the two-hinge chain (with just two hinges meeting at vertex $P = p_{i+1}$) coincide.

Relation (1) follows easily from the fact that, in the planar configuration C, the sum of the lengths of the segments $[SQ]$ and $[QT]$ is at least $|SP| + |PT|$, since Q is not in the interior of the ellipse, while each segment length is less or equal with the maximum reach of the corresponding subchain. $\square$

This theorem shows that when we know that a plygonal chain ST has a flat maximal configuration C, we can reconstruct this maximal configuration based on information relating only to maximal reaches of proper subchains. Indeed, we find first a proper vertex P such that

$$Max\{SP\} + Max\{PT\} \leq Max\{SQ\} + Max\{QT\} \quad (2)$$

for all proper vertices Q. Then P must be on the empty ellipse of the maximal flat configuration C, hence the sub-

(a) A flat maximum reach configuration. The ellipse through P, with foci at S and T has no intersection of consecutive hinges in its interior.

(b) A flat minimum reach configuration dual to a flat maximum reach configuration of the type illustrated in (a).
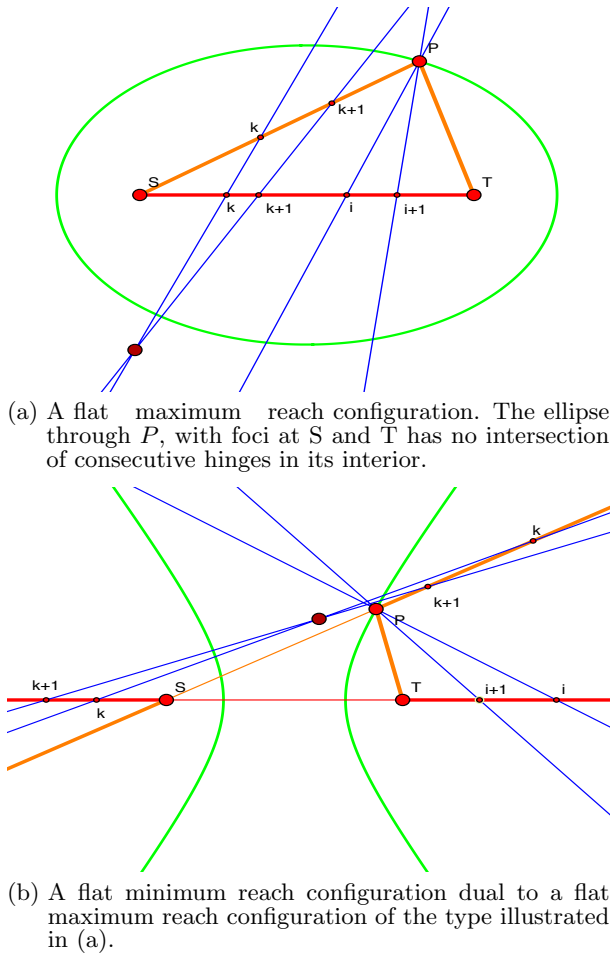
Figure 7: A projective transformation between an ellipse and a hyperbola. This turns the correctness proof for max reach into a correctness proof for min reach.

chains SP and PT must have flat maximal reaches. We lock them in their maximal flat configurations and then obtain, by the two-hinge rule, the flat maximal configuration C.

Figure 8 illustrates three chains in flat maximal reach configurations and shows the corresponding 'empty ellipses'.

We turn now to the main algorithmic results.

4. THE MAXIMUM REACH ALGORITHM

The overall idea and structure of our polynomial time algorithm can now be described. The structural *empty ellipse* property of maximum reach, proven in Theorem 3.1, leads directly to the following recursive algorithm:

ALGORITHM 1. **Maximum Reach (Recursive Version)**
Input: *A 3D chain $p = \{p_0, p_1, \cdots, p_{n+1}, p_{n+2}\}$, $n \geq 0$.*
Output: *The value of the maximum reach between the chain endpoints and a max reach configuration.*
Method:
Base cases. *If $n = 0$ (no hinge), there is only one possible configuration of the chain, which is of course maximum. If $n = 1$ (one hinge), the maximum is reached in a flat configuration, with $S = p_0$ and $T = p_3$ on opposite sides of the hinge $p_1 p_2$. When $n = 2$ (two hinges), compute the maximum reach in constant time.*

Recursive step.
[1]. For each vertex p_i of the chain which is the intersection of two hinges, i.e. for $i = 2, \cdots, n$:
[1a]. Compute recursively the maximum reaches M_i^L and M_i^R of the two subchains $L_i = \{p_0, \cdots, p_i\}$ and $R_i = \{p_i, \cdots, p_{n+2}\}$.
[1b]. Compute the sum $S_i = M_i^L + M_i^R$.
[2]. Compute an index i achieving the minimum of S_i (if there is a tie, choose any of them), as well as maximum reach configurations C_i^L and C_i^R. "Freeze" these configurations, i.e. consider them as rigid bodies. The endpoint p_0 and the hinge axis $p_{i-1}p_i$, resp. the axis $p_i p_{i+1}$ and the endpoint p_{n+2}, induce two panels P_i^L and P_i^R rigidly attached to these bodies. They are also rigidly attached to the concurrent hinges $p_{i-1}p_i$ and $p_i p_{i+1}$, inducing a short panel-and-hinge chain $q_i = \{p_0, p_{i-1}, p_i, p_{i+1}, p_{n+2}\}$ with exactly two hinges.
[3]. Compute the maximum reach of the 2-hinged chain q_i, and output its value as the maximum reach value for the original chain p. To obtain a maximum reach configuration, overlay the frozen bodies C_i^L and C_i^R over their corresponding panels P_i^L and P_i^R in the max reach configuration of q_i. In particular, if vertex p_i was a fold point in the chain q_i, it will be a fold point in the large chain p. Otherwise, the flattening pattern at p_i in the small chain, is retained in the large chain.

The algorithm is not yet polynomial, due to superfluous recursive calls. For the Dynamic programming version, we maintain an array $A = (a_{ij})$ whose entries store the maximum reach information (value and configuration) for chains $c_{ij} = \{p_i, \cdots, p_j\}$. Then we just follow the steps of the recursive algorithm, but when computing the entry for a_{ij}, instead of recursively calling the algorithm, we look up the entries for a_{ik} and a_{kj}, $i \leq k \leq j$, which have previously been computed and stored.

Complexity of the algorithm. The base case of $n \leq 2$ hinges takes constant time. Each entry a_{ij} requires $O(j-i)$ steps to compute the minimum sum. This leads to an overall $O(n^3)$ time and $O(n^2)$ space complexity for intermediate max reach values (some care is needed in storing the intermediate max reach configurations, but we defer these details to the full paper).

Finally, we turn to correctness.

THEOREM 4.1. *Algorithm 1 correctly computes the Maximum Reach, for generic chains.*

PROOF. In Step [3] of the algorithm, the maximum reach for the small 2-hinge chain q_i either leads to a fold point at p_i or is flat. In the first case, the correctness is straightforward: by induction we assume that the maximum was computed correctly for the two subchains L_i and R_i; the endpoint axes of the two subchains, $p_0 p_i$ and $p_i p_{n+2}$, correctly cross the axes in the two subchains, and when they get aligned (in q_i), this leads to global natural order. Notice that if the maximum reach has several fold points, the minimum sum in Step [2] will be achieved at all of them. The fact that each choice is correct is straightforward. The proof reduces to the case when there are no fold points, i.e. the max reach of p is flat, which follows from Theorem 3.1 above. □

5. THE MINIMUM REACH ALGORITHM

We describe now the algorithm for minimum reach. This part is self-contained but the interested reader may find a more detailed and intuitive discussion of (non-zero) minimum configurations for orthogonal chains in [4].

Our algorithm will detect if the minimum reach value is zero or non-zero and will obtain a minimum reach configuration for the non-zero case. As we already indicated in
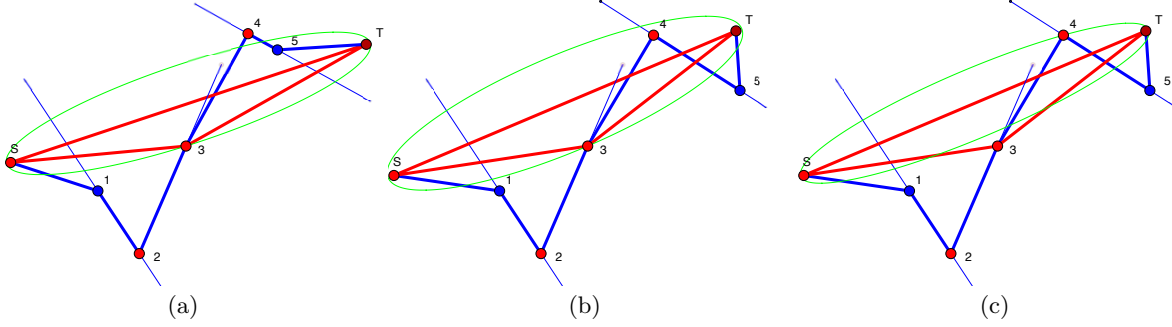
Figure 8: (a) In a flat max reach configuration, the ellipse with foci at S and T, going through the point p_i computed in Step 2, does not contain any other intersections of hinge axes. Notice that p_1 and p_{n+1} are not proper vertices (i.e. intersections of hinges), and for them there is no restriction on being inside the ellipse. (b) For a slightly different chain, vertex 3 does not have an empty ellipse, although the chain is in a maximum reach position, but (c) the ellipse is empty at vertex 4, where the minimum of the sums S_i from step **2** is achieved.

the Introduction, the zero-case is special: the configurations achieving it will be, in general, a high dimensional variety, not a discrete set as in the non-zero case. Selecting any one of them is an instance of *inverse kinematics*, a related problem which falls outside the scope of this paper.

ALGORITHM 2. **Minimum Reach (Recursive Version)**
Input: *A 3D chain* $p = \{p_0, p_1, \cdots, p_{n+1}, p_{n+2}\}$, $n \geq 0$.
Output: *The value of the minimum reach between the chain endpoints and the collection of* fold *points.*
Method:
Base case. *If* $n = 0$ *(no hinge), there is only one possible configuration of the chain, which is of course maximum. If* $n = 1$ *(one hinge), the minimum is reached in a flat configuration, with* $S = p_0$ *and* $T = p_3$ *on opposite sides of the hinge* $p_1 p_2$. *When* $n = 2$ *(two hinges), compute the minimum reach in constant time.*
Recursive step.
[1]. For each vertex p_i *of the chain which is the intersection of two hinges, i.e. for* $i = 2, \cdots, n$:
[1a]. Compute recursively the maximum reaches M_i^L *and* M_i^R *of the two subchains* $L_i = \{p_0, \cdots, p_i\}$ *and* $R_i = \{p_i, \cdots, p_{n+2}\}$.
[1b]. Compute recursively the minimum reaches m_i^L *and* m_i^R *of the two subchains* $L_i = \{p_0, \cdots, p_i\}$ *and* $R_i = \{p_i, \cdots, p_{n+2}\}$.
[1c]. Compute the differences $D_i^S = m_i^L - M_i^R$ *and* $D_i^T = M_i^L - m_i^R$.
[2]. Compute an index i *achieving the maximum* M *of* D_i^S *and* D_i^T, *for all* i's *(if there is a tie, choose any of them), and, if* $M > 0$, *also the minimum, resp. maximum reach configurations* C_i^L *and* C_i^R.
If $M < 0$, *we conclude that the minimum reach value is zero. (No particular minimum reach configuration is provided by the algorithm in this case.)*
Otherwise, we "freeze" these configurations, i.e. consider them as rigid bodies. The endpoint p_0 *and the hinge axis* $p_{i-1} p_i$, *resp. the axis* $p_i p_{i+1}$ *and the endpoint* p_{n+2}, *induce two panels* P_i^L *and* P_i^R *rigidly attached to these bodies. They are also rigidly attached to the concurrent hinges* $p_{i-1} p_i$ *and* $p_i p_{i+1}$, *inducing a short panel-and-hinge chain* $q_i = \{p_0, p_{i-1}, p_i, p_{i+1}, p_{n+2}\}$ *with exactly two hinges.*
[3]. Compute the minimum reach of the short chain q_i, *and output its value as the minimum reach value for the original chain* p. *To obtain a minimum reach configuration, when the minimum reach is non-zero, overlay the frozen bodies* C_i^L *and* C_i^R *over their corresponding panels* P_i^L *and* P_i^R *in the max reach configuration of* q_i. *In particular, if vertex* p_i *was a fold point in the chain* q_i, *it will be a fold point in the large chain* p. *Otherwise, the flattening pattern at* p_i *in the small chain, is retained in the large chain.*

Note that $M > 0$ always implies a non-zero minimum reach. It will be seen from subsequent arguments that (under our genericity assumption) the case $M = 0$ can occur only for $n = 2$.

THEOREM 5.1. *Algorithm 2 correctly computes the Minimum Reach, for generic chains.*

The reader may observe the symmetry between the Max and Min Reach algorithms. The proof of correctness for the minimum could proceed in a similar fashion as for the maximum. However, a more elegant argument is obtained via a projective transformation.

PROOF. It suffices to treat the case with no fold points (otherwise, the proof is similar to the one for the maximum). We show that the flat extremal cases are related by a projective duality transformation. In adequate coordinates, the duality transformation takes the form: $(x, y) \rightarrow (\frac{1}{x}, \frac{y}{x})$, $S = (-1, 0)$, $T = (1, 0)$. Indeed, this projective transformation takes the line $y = 0$ through $S = (-1, 0)$ and $T = (1, 0)$ to itself, but exchanges the affine segment $[S, T]$ with the segment from S to T passing through the point at infinity. In essence, this means that a Minimum configuration is transformed into a Maximum configuration, which justifies the conclusion. We remind the reader that the ellipse is the locus of points with constant sum of distances to the two foci, while the hyperbola uses the difference, which justifies the calculations performed by the algorithms.

The line $x = 0$ is exchanged with the line at infinity and the family of *ellipses* with foci at S and T: $(1 - \frac{1}{\lambda^2})x^2 + y^2 = \lambda^2(1 - \frac{1}{\lambda^2})$, $\lambda \geq 1$ with the family of *hyperbolas*: $\lambda^2(1 - \frac{1}{\lambda^2})x^2 - y^2 = (1 - \frac{1}{\lambda^2})$, $\lambda \geq 1$ The ellipse in Figure 7(a) corresponds to $SP + PT = 2\lambda$ and the hyperbola in Figure 7(b) corresponds to $|SP - PT| = 2(1 - 1/\lambda)$. □

Complexity of the algorithm. Using an additional array data structure, the recursive algorithm can be implemented with dynamic programming to yield an efficient solution for Min Reach, with overall $O(n^3)$ time and $O(n^2)$ space complexity. The analysis is identical to the one for Max Reach.

6. CONCLUDING REMARKS

We have presented the first polynomial time algorithm for the Maximum and Minimum Reach of arbitrary polygonal chains. We conclude by formulating the following:

Conjecture: *The Extremal Reaches Problem, for general body-and-hinge chains, is NP-hard.*

Any upper bound, even an exponential one, for either the Maximum or the Minimum Reach would be an important theoretical advance. So far no known methods, even approximate numerical ones, are guaranteed to compute the (generically unique) global maximum in this case: the gradient-based methods may get stuck in local maxima, and Monte Carlo methods may hop between local maxima with no criterion to guide them toward the global maximum. Note, however, that our natural-order criterion would allow these methods to decide, when in a local maximum, whether it is or not the global one. As we indicated in Section 2, no such criterion exists for the global minimum of *arbitrary* body-and-hinge chains. It remains an open problem to elucidate the theoretical underpinnings of this intriguing asymmetry between the maximum and minimum reach in the general case.

References

[1] Karim Abdel-Malek, Jingzhou Yang, and Yunqing Zhang. On the workspace boundary determination of serial manipulators with non-unilateral constraints. *Robotics and Computer-Integrated Manufacturing*, 24:60–76, 2008.

[2] Greg Aloupis, Erik D. Demaine, Vida Dujmovic, Jeffrey Gordon Erickson, Stefan Langerman, Henk Meijer, Joseph O'Rourke, Mark Overmars, Michael A. Soss, Ileana Streinu, and Godfried T. Toussaint. Flat state connectivity of linkages under dihedral motions. In *Proc. 13th Annual Internat. Symp. Algorithms and Computation (ISAAC'02)*, pages 369–380, November 2002.

[3] Greg Aloupis, Erik D. Demaine, Henk Meijer, Joseph O'Rourke, Ileana Streinu, and Godfried T. Toussaint. Flat-state connectivity of chains with fixed acute angles. In *Proceedings of the 14th Canadian Conference on Computational Geometry (CCCG 2002)*, pages 27–30, Lethbridge, Alberta, Canada, 2002.

[4] Ciprian Borcea and Ileana Streinu. Exact workspace boundary by extremal reaches. In these proceedings, SoCG, 2011.

[5] Ciprian S. Borcea and Ileana Streinu. Extremal configurations of manipulators with revolute joints. In *Reconfigurable Mechanisms and Robots, Proc. ASME/IFToMM International Conference (ReMAR'09), Jian S. Dai, Matteo Zoppi and Xianwen Kong (eds.), King's College, London, UK*, pages 279–284. KC Edizioni, June 2009. arXiv:0812.1375.

[6] Ciprian S. Borcea and Ileana Streinu. How far can you reach? In *Proc. ACM-SIAM Symposium on Discrete Algorithms (SODA10)*, pages 928–937, January 2010.

[7] John F. Canny and David Parsons. Geometric problems in molecular biology and robotics. In *Proceedings of the Second International Conference on Intelligent Systems for Molecular Biology, Stanford, CA*. August 1994.

[8] Erik D. Demaine and Joseph O'Rourke. *Geometric Folding Algorithms: Linkages, Origami, and Polyhedra.* Cambridge University Press, 2007.

[9] Stephen Derby. The maximum reach of revolute jointed manipulators. *Mechanism and Machine Theory*, 16(3):255–261, 1981.

[10] James Urey Korein. *A geometric investigation of reach.* MIT Press, Cambridge, MA, June 1985.

[11] A. Kumar and K. J. Waldron. The workspaces of a mechanical manipulator. *Journal of Mechanical Design*, 103(3):665–672, 1981.

[12] Scott B. Nokleby. Singularity analysis of the Canadarm2. *Mechanism and Machine Theory*, 42(4):442–454, April 2007.

[13] Andres Oberhauser and Mariano Carrion-Vazquez. Mechanical biochemistry of proteins one molecule at a time. *Journal of Biological Chemistry*, 283(11):6617–6621, March 2008.

[14] Robert J. Schilling. *Fundamentals of Robotics.* Prentice Hall, 1990.

[15] R. G. Selfridge. The reachable volume of a robot arm. In *Proceedings of the 20th Annual Southeast Regional Conference, 1982*, pages 110–114. ACM, April 1982.

[16] R. G. Selfridge. The reachable workarea of a manipulator. *Mechanism and Machine Theory*, 18(2):131–137, 1983.

[17] Michael A. Soss. *Geometric and computational aspects of molecular reconfiguration.* Phd thesis, School Comput. Science, McGill University, 2001.

[18] Michael A. Soss and Godfried T. Toussaint. Geometric and computational aspects of polymer reconfiguration. *Journal of Mathematical Chemistry*, 27(4):303–318, 2000.

[19] K. Sugimoto and Joseph Duffy. Determination of extreme distances of a robot hand - Part 1 : A general theory. *Journal of Mechanical Design*, 103(3):631–636, 1981.

[20] H van den Bedem, Itay Lotan, Jean-Claude Latombe, and A. M. Deacon. Real-space protein-model completion: an inverse kinematics approach. *Acta Crystallographica Section D*, D61:2–13, 2005.